

Electric multipole moments, polarizability, and hyperpolarizability of xenon dihydride (HXeH)

George Maroulis

Received: 21 October 2010 / Accepted: 7 December 2010 / Published online: 28 December 2010
© Springer-Verlag 2010

Abstract We report an extensive theoretical investigation of the electric moments and dipole (hyper)polarizability of xenon dihydride. We have employed conventional ab initio and DFT methods and large, flexible Gaussian-type basis sets. Our best values for the electric moments are obtained at the CCSD level of theory and are $\Theta = -4.8760 \text{ } ea_0^2$ and $\Phi = -71.95 \text{ } ea_0^4$. For the (hyper)polarizability, our best results, extracted from finite-field CCSD(T) calculations, are $\bar{\alpha} = 49.93$ and $\Delta\alpha = 55.80 \text{ } e^2 a_0^2 E_h^{-1}$, for the mean and the anisotropy of the dipole polarizability and $\bar{\gamma} = 31.26 \times 10^3 e^4 a_0^4 E_h^{-3}$ for the mean second hyperpolarizability. Overall, the molecule is characterized by large (hyper)polarizability anisotropies. The DFT methods predict dipole polarizabilities comparable to those calculated by ab initio but overestimate the second hyperpolarizability.

Keywords Xenon dihydride · Quadrupole moment · Hexadecapole moment · Electric dipole polarizability · Electric dipole hyperpolarizability

1 Introduction

The chemistry of xenon compounds has attracted considerable attention in late years, both experimentally [1–3] and theoretically [4]. Most work has focused on the spectroscopic properties and molecular structure. Little has

been done on the electric properties of xenon compounds [5, 6], although recent significant work seems to bring forth the need for accurate values of their polarizability [7]. In this work, we concentrate on the electric multipole moments, polarizability, and hyperpolarizability of the prototypical xenon compound, the dihydride XeH_2 (HXeH). The synthesis and identification of XeH_2 have been reported by Pettersson et al. [8], Lundell et al. [9] and Lorenz et al. [10]. Khriachtchev et al. [11] have provided experimental evidence of the solid-phase $\text{H} + \text{HXeH}$ reaction. Feldman et al. [12] measured the xenon isotopic shift in the IR spectra of xenon hydrides. Important theoretical work has been reported on XeH_2 . An early theoretical investigation of XeH_2 was published by Runeberg et al. [13]. Lundell et al. [14] calculated the molecular structure and spectra of dihydrogen-bonded complexes of XeH_2 with H_2O . A study of XeH_2 as a proton acceptor in dihydrogen-bonded complexes was presented by Solimannejad et al. [15]. Lundell et al. [16] studied the molecular structure and spectra of the $(\text{HXeH})_2$ dimer. Clusters up to $(\text{HXeH})_4$ have also been studied (see the extensive review by Gerber, cited above, who also mentions advanced work on the crystal structure of XeH_2). Takayanagi et al. [17] reported a 3D potential energy surface for XeH_2 and calculated vibrational energy levels of HXeH , HXeD , and DXeD . Blanco et al. [18] explored the formation of inverse hydrogen bonds between XeH_2 and hydrides and fluorides of Li, Be, Na, and Mg. Last, the interaction of xenon dihydride with halogen donor molecules and the formation of halogen-bonded complexes were reported by Solimannejad et al. [19]. Our aim is to obtain accurate values for the electric moments and the electric dipole (hyper)polarizability. These properties are of fundamental importance to intermolecular interaction studies [20], non-linear optics [21], collision-induced

Dedicated to Professor Pekka Pyykkö on the occasion of his 70th birthday and published as part of the Pyykkö Festschrift Issue.

G. Maroulis (✉)
Department of Chemistry, University of Patras,
26500 Patras, Greece
e-mail: maroulis@upatras.gr

spectroscopy [22], and the simulation of fluids [23]. They are also routinely associated with general molecular characteristics as hardness [24], softness [25], hypersoftness [26], stiffness [27], and compressibility [28].

The electric properties of interest in this work are the quadrupole (Θ) and hexadecapole (Φ) moment, the dipole (α) polarizability and second (γ) hyperpolarizability. The electric moments for a given level of theory are extracted from the respective density [29]. The finite-field method is used for the calculation of the (hyper)polarizability. This computationally economic method, coupled with a suitable choice of flexible, purpose-oriented, Gaussian-type function (GTF) basis sets has been shown to perform successfully for a large class of systems, from atoms [30] and molecules [31, 32] to clusters [33, 34] of some size. We employ conventional ab initio methods and density functional theory (DFT)-based approaches. We are particularly interested in enriching the already available knowledge [35–38] as regards the relative importance of widely used DFT methods in electric property calculations. In this work, we present a rigorous analysis of their performance. DFT methods are now extensively used in such investigations, although there is no consensus on their predictive capability. We rely on a generalized metric approach that combines a graph-theoretic background and pattern recognition techniques to introduce proximity, similarity, classification, and clustering in spaces of theoretical descriptions of molecules. This method, previously introduced by us [39], is now variously used in the analysis of the results of theoretical investigations [40–44]. In this work, it is used for the study of basis set effects and the quantitative analysis of the performance of DFT methods in comparison with conventional ab initio quantum chemical methods.

2 Theory and computational perspective

The energy of an uncharged molecule in a weak, static electric field is given by the expansion [45, 46]

$$\begin{aligned} E^p &\equiv E^p(F_\alpha, F_{\alpha\beta}, F_{\alpha\beta\gamma}, F_{\alpha\beta\gamma\delta}, \dots) \\ &= E^0 - \boldsymbol{\mu}_\alpha F_\alpha - (1/3)\boldsymbol{\Theta}_{\alpha\beta} F_{\alpha\beta} - (1/15)\boldsymbol{\Omega}_{\alpha\beta\gamma} F_{\alpha\beta\gamma} \\ &\quad - (1/105)\boldsymbol{\Phi}_{\alpha\beta\gamma\delta} F_{\alpha\beta\gamma\delta} + \dots \\ &\quad - (1/2)\boldsymbol{\alpha}_{\alpha\beta} F_\alpha F_\beta - (1/3)\boldsymbol{A}_{\alpha\beta\gamma} F_\alpha F_{\beta\gamma} - (1/6)\boldsymbol{C}_{\alpha\beta\gamma\delta} F_\alpha F_{\beta\gamma\delta} \\ &\quad - (1/15)\boldsymbol{E}_{\alpha\beta\gamma\delta} F_\alpha F_{\beta\gamma\delta} + \dots \\ &\quad - (1/6)\boldsymbol{\beta}_{\alpha\beta\gamma} F_\alpha F_\beta F_\gamma - (1/6)\boldsymbol{B}_{\alpha\beta\gamma\delta} F_\alpha F_\beta F_{\gamma\delta} + \dots \\ &\quad - (1/24)\boldsymbol{\gamma}_{\alpha\beta\gamma\delta} F_\alpha F_\beta F_\gamma F_\delta + \dots \end{aligned} \quad (1)$$

where F_α , $F_{\alpha\beta}$, $F_{\alpha\beta\gamma}$, etc. are the field, field gradient, etc. at the origin. E^0 is the energy of the unperturbed molecule and the expansion coefficients (in bold) are the first- ($\boldsymbol{\mu}_\alpha$, $\boldsymbol{\Theta}_{\alpha\beta}$, $\boldsymbol{\Omega}_{\alpha\beta\gamma}$ and $\boldsymbol{\Phi}_{\alpha\beta\gamma\delta}$), second- ($\boldsymbol{\alpha}_{\alpha\beta}$, $\boldsymbol{A}_{\alpha\beta\gamma}$, $\boldsymbol{E}_{\alpha\beta\gamma\delta}$, $\boldsymbol{C}_{\alpha\beta\gamma\delta}$), third-

($\boldsymbol{\beta}_{\alpha\beta\gamma}$, $\boldsymbol{B}_{\alpha\beta\gamma\delta}$) and fourth-order ($\boldsymbol{\gamma}_{\alpha\beta\gamma\delta}$) properties. The subscripts denote Cartesian components and a repeated subscript implies summation over x, y, and z.

For a centrosymmetric molecule, as HXeH, $\boldsymbol{\mu}_\alpha = \boldsymbol{\Omega}_{\alpha\beta\gamma} = \boldsymbol{A}_{\alpha\beta\gamma} = \boldsymbol{E}_{\alpha\beta\gamma\delta} = 0$. This results in a significant reduction in the size of the expansion of Eq. 1. In the case of a homogeneous field, the expansion of Eq. 1 reduces further to

$$E^p = E^0 - (1/2)\boldsymbol{\alpha}_{\alpha\beta} F_\alpha F_\beta - (1/24)\boldsymbol{\gamma}_{\alpha\beta\gamma\delta} F_\alpha F_\beta F_\gamma F_\delta + \dots \quad (2)$$

The number of independent components needed to specify the dipole tensors is dictated by symmetry. Our choice of independent components follows previous work [47]. With z as the molecular axis, there is only one non-vanishing component for the electric moments, $\boldsymbol{\Theta}_{\alpha\beta} \equiv \boldsymbol{\Theta}$ and $\boldsymbol{\Phi}_{\alpha\beta\gamma\delta} \equiv \boldsymbol{\Phi}$. For $\boldsymbol{\alpha}_{\alpha\beta}$, we pick α_{zz} , α_{xx} and for $\boldsymbol{\gamma}_{\alpha\beta\gamma\delta}$, γ_{zzzz} , γ_{xxxx} , γ_{xxzz} . In addition to the Cartesian components, we compute also the following invariants:

$$\begin{aligned} \bar{\alpha} &= (\alpha_{zz} + 2\alpha_{xx})/3 \\ \Delta\alpha &= \alpha_{zz} - \alpha_{xx} \\ \bar{\gamma} &= (3\gamma_{zzzz} + 8\gamma_{xxxx} + 12\gamma_{xxzz})/15 \\ \Delta_1\gamma &= 3\gamma_{zzzz} - 4\gamma_{xxxx} + 3\gamma_{xxzz} \\ \Delta_2\gamma &= \gamma_{zzzz} + \gamma_{xxxx} - 6\gamma_{xxzz} \end{aligned}$$

The conventional ab initio methods used in this work are the following:

SCF	self-consistent field
MP2	second-order Møller-Plesset perturbation theory (MP)
MP3	third-order MP
SDQ-MP4	partial fourth-order MP
MP4	complete fourth-order Møller-Plesset perturbation theory
CCSD	singles and doubles coupled cluster, and
CCSD(T)	which includes an estimate of connected triples via a perturbational treatment. The MP3 method is rarely used now in theoretical investigations. It is included here only for reasons of completeness.

The interested reader will find extensive presentations of the above-mentioned methods in standard references [48–51]. Of all methods used in this work, CCSD(T) is presumably the one with the highest predictive capability. We define the total electron correlation correction (ECC) as,

$$\text{ECC} = \text{CCSD}(T) - \text{SCF} \quad (4)$$

The DFT methods employed here are B3LYP, B3PW91 and mPW1PW91, as implemented in GAUSSIAN 03 [52]. A detailed description of their composition is given elsewhere [53].

Our approach to the rigorous analysis of the performance of theoretical methods relies on graph theoretical

arguments and pattern recognition techniques. It has been presented in some detail elsewhere [39]. A generalized metric is used to define proximity between theoretical descriptions of molecules. A theoretical description is essentially an n -dimensional object, defined as follows. Let $Q_{m\alpha}$ be the value of the molecular property α (taking values in the index set I_A) calculated with method m (taking values in I_M)

$$Q_{m\alpha}, m \in I_M (\text{methods}), \alpha \in I_A (\text{properties}) \quad (5)$$

The theoretical description of the molecule associated with method i , TD_i , is a collection of values that is an n -dimensional object defined as

$$\text{TD}_i = \{Q_{i\alpha}, \alpha \in I_A\} \quad (6)$$

Distance or proximity in the space of all theoretical descriptions (TD) is defined using a generalized form of the Minkowski metric. The distance between TD_i and TD_j is defined as

$$D_{ij} = \left(\sum_{\alpha} \frac{|Q_{i\alpha} - Q_{j\alpha}|^p}{(\max_{ij} |Q_{i\alpha} - Q_{j\alpha}|)^p} \right)^{1/p}, \quad p \geq 1 \quad (7)$$

Similarity between two theoretical descriptions TD_i and TD_j is defined on the basis of proximity as

$$S_{ij} = 1 - \frac{D_{ij}}{\max_{ij} D_{ij}}, \quad 0 \leq S_{ij} \leq 1 \quad (8)$$

Let us consider G with vertex set $V(G) = \{\text{TD}_i, i \in I_M\}$ and as the edge set $E(G)$, a subset of the Cartesian product $\text{TD} \times \text{TD}$. We define a generalized distance on G by assigning to each edge $e = \{\text{TD}_i, \text{TD}_j\}$ a weight equal to the distance D_{ij} . The minimum spanning tree (MST) of G is a spanning tree for which the sum of the weights of the edges is minimal [54]. Clustering is then achieved by removing from MST all edges with weights greater than a given threshold D_T . This method of clustering is called single linkage cluster analysis (SLCA) [55].

3 Basis sets and other computational details

The search for Gaussian basis sets suitable for molecular property calculations is vital to computational quantum chemistry [56–58]. The construction of molecule-specific, purpose-oriented basis sets for large molecular architectures, or low-symmetry polyatomics is largely impractical. Nevertheless, previous work shows that for systems of reasonable size as atoms [59], diatomics [60, 61] and triatomics [62], symmetric polyatomics [63, 64], clusters [65, 66] and interacting atom–atom [67], atom–molecule [68] or molecule–molecule [69] pairs, one can easily control the

construction of the basis set in order to obtain suitable basis sets for electric property calculations.

In this paper, leaning heavily on previous findings, we have chosen the following basis sets for our calculations on XeH_2 . In brief, their composition has as follows:

B1 = [9s8p7d1f/4s2p] for Xe/H . The Xe part is a flexible, optimized basis set taken from our work on Xe dimer [70]. The H part was built on a [3s] substrate from the Karlsruhe Database [71] and optimized to [4s2p] on the H_2 molecule [72]. The composition of this basis is [4s2p] = [3s] + s(0.0324662) + p(0.9559, 0.1268).

B2 = [9s8p7d1f/4s3p1d]

$$= \text{B1} + \text{H}: p(0.3481) + d(0.1268)$$

B3 = [9s8p7d5f1g/4s3p1d]. The Xe part is taken from Ref. [70].

B4 = [9s8p7d5f1g/6s4p3d1f]. The H part is an augmented version of the [6s4p2d] basis used on the interaction (hyper)polarizability of the $\text{H}_2\text{-Ar}$ pair [73]. The additional functions are [6s4p3d1f] = [6s4p2d] + d(0.1246) + f(0.1246).

Last, two very large basis sets **B5** and **B6** were used to check to a certain extent the convergence of the calculated values.

B5 = [15s12p9d3f/14s8p5d]. The Xe part of this basis has been built upon a [14s11p6d] substrate taken from the Karlsruhe database. The composition of this part is [15s12p9d3f] = [14s11p6d] + s(0.0539934) + p(0.0383211) + d(0.2671, 0.1024, 0.0393) + f(0.3069, 0.1023, 0.0341). The H part was taken from previous work on the interaction (hyper)polarizability of the $\text{H}_2\text{-He}$ pair [74].

B6 = [15s12p9d7f1g/14s8p5d], where [15s12p9d7f1g] = [15s12p9d3f] + f(0.9207, 0.1772, 0.0591, 0.0114) + g(0.1023).

5D, 7F and 9G GTF were used on all basis sets.

A theoretical molecular geometry was used in this work. It is defined by a Xe–H bond length of 1.8767226454 Å obtained at the MP2(FULL) level of theory with a basis set consisting of $\text{Xe} = [9s8p7d1f]$ (see **B1** earlier) and the standard cc-pvdz basis set for H. All subsequent calculations were performed with GAUSSIAN 03.

Atomic units are used throughout this paper. Conversion factors to SI units are, Energy, $1 E_h = 4.3597482 \times 10^{-18}$ J, Length, $1 a_0 = 0.529177249 \times 10^{-10}$ m, Θ , $1 ea_0^2 = 4.486554 \times 10^{-40}$ Cm², Φ , $1 ea_0^4 = 1.256363 \times 10^{-60}$ Cm⁴, α , $1 e^2 a_0^2 E_h^{-1} = 1.648778 \times 10^{-41}$ C²m²J⁻¹ and γ , $1 e^4 a_0^4 E_h^{-3} = 6.235378 \times 10^{-65}$ C⁴m⁴J⁻³. Property values are mostly given as pure numbers, that is Θ/ea_0^2 , $\alpha/e^2 a_0^2 E_h^{-1}$, etc.

4 Results and discussion

All post-Hartree–Fock calculations were performed with the 18 innermost MO kept frozen. To test this approximation, we calculated the dipole polarizability at the MP2/**B3** level of theory successively reducing the frozen core. Thus, we find that the mean $\bar{\alpha}$ varies as 52.77(FC = 18), 52.77 (FC = 9), 52.72(FC = 5), 52.72(FC = 1), 52.72(FULL) with increasing number of correlated electrons. The change is quite small.

4.1 Electric multipole moments

SCF, MP2, and CCSD values for the electric moments of XeH₂ are given in Table 1. Only SCF and MP2 values were calculated with the large **B5** and **B6** basis sets. Our best SCF values for Θ and Φ are –5.2716 and –72.90, respectively. We observe a smooth converge of the SCF values for the sequence **B1** → **B6**. Electron correlation reduces the magnitude of both moments for **B6**. The effect is rather small for both properties. The CCSD values obtained with the large **B4** basis show that increasing the level of theory has a much stronger effect for Θ than it has for Φ .

In Table 2, we display SCF, MP2, and CCSD values for both moments calculated with basis set **B3** for the symmetric stretch of the Xe–H bond in the range $-0.3 \leq (R-R_e)/\text{Å} \leq 0.2$. The R-dependence of the moments is also plotted in Figs. 1 and 2. The electron correlation effect does not vary uniformly with increasing bond length. Hence, the significant differentiation of the MP2 and CCSD curves from the SCF one for relatively large distances. We have obtained the first derivative of both moments at R_e from a polynomial fit of the respective curves. The resulting $D^1P \equiv (\frac{dP}{dR})_e$ values are given in Table 3. Significant variation is observed for $D^1\Theta$.

4.2 Dipole polarizability

R_e values for the dipole polarizability of XeH₂ are shown in Table 4. The molecule has very large dipole polarizability anisotropy as the longitudinal component α_{zz} is significantly larger than the transversal one α_{xx} . Our best SCF/**B6** values for the invariants are $\bar{\alpha} = 53.33$ and $\Delta\alpha = 67.95$. The SCF/**B4** values are quite close to the SCF/**B6** ones. We note that the SCF/**B1** values are only 1.01 below and 1.25% above the most accurate SCF/**B6** results. Electron correlation has a strong effect on the longitudinal and a rather small effect on the transversal component of the dipole polarizability. The ECC is –11.51 and 0.66, for α_{zz} and α_{xx} , respectively. Consequently, both invariants $\bar{\alpha}$ and $\Delta\alpha$ decrease with electron correlation. The effect is not uniform. MP2 seems to differ considerably from the other methods.

Table 1 Electric moments of XeH₂ at the equilibrium molecular geometry

Basis set	Method	Θ	Φ
B1	SCF	–5.1919	–74.72
	MP2	–5.3116	–77.99
	CCSD	–5.0292	–77.53
B2	SCF	–5.1763	–70.98
	MP2	–5.2384	–73.24
	CCSD	–4.9913	–73.16
B3	SCF	–5.2444	–71.19
	MP2	–5.1264	–70.44
	CCSD	–4.8762	–70.49
B4	SCF	–5.2529	–73.47
	MP2	–5.1261	–71.86
	CCSD	–4.8760	–71.95
B5	SCF	–5.2513	–72.96
	MP2	–5.1100	–70.50
B6	SCF	–5.2716	–72.90
	MP2	–5.1749	–69.82

Table 2 Xe–H bond length dependence of the electric moments of XeH₂ at the equilibrium molecular geometry calculated with basis set **B3**

$(R-R_e)/\text{\AA}$	Θ			Φ		
	SCF	MP2	CCSD	SCF	MP2	CCSD
–0.30	–3.9379	–4.3521	–4.1858	–73.46	–74.25	–73.03
–0.25	–4.2237	–4.5659	–4.3952	–73.07	–73.56	–72.55
–0.20	–4.4799	–4.7435	–4.5662	–72.72	–72.94	–72.13
–0.15	–4.7085	–4.8870	–4.6998	–72.39	–72.35	–71.75
–0.10	–4.9113	–4.9980	–4.7964	–72.05	–71.76	–71.37
–0.05	–5.0896	–5.0776	–4.8555	–71.66	–71.14	–70.96
0	–5.2444	–5.1264	–4.8762	–71.19	–70.44	–70.49
0.05	–5.3768	–5.1445	–4.8572	–70.62	–69.66	–69.93
0.10	–5.4875	–5.1322	–4.7969	–69.93	–68.78	–69.25
0.15	–5.5769	–5.0888	–4.6939	–69.10	–67.79	–68.45
0.20	–5.6456	–5.0137	–4.5474	–68.11	–66.70	–67.52

In Table 5, we give the R-dependence of the dipole polarizability components for the symmetric stretching of the Xe–H bond. The SCF and MP2 values have been obtained with basis **B4** and the CCSD ones with basis **B3**. The R-dependence of the invariants is plotted in Fig. 3. For small values of the displacement parameter ($R-R_e$), the MP2 method gives a positive electron correlation effect while the opposite is observed for the CCSD one. This discrepancy is not present for $(R-R_e) > 0$, as for this range, both methods predict a negative electron correlation effect. The calculated D^1P derivative values for both invariants are listed in Table 6. The SCF values of $D^1\bar{\alpha}$ and

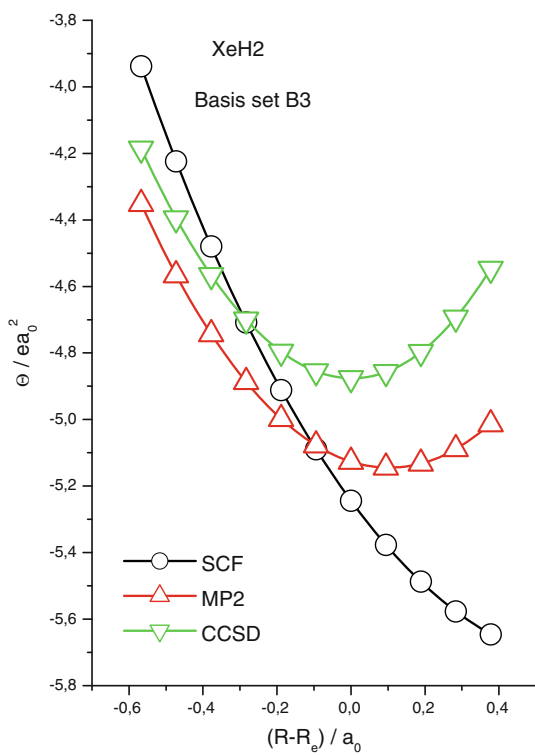


Fig. 1 Xe–H bond length dependence of the quadrupole moment of XeH_2

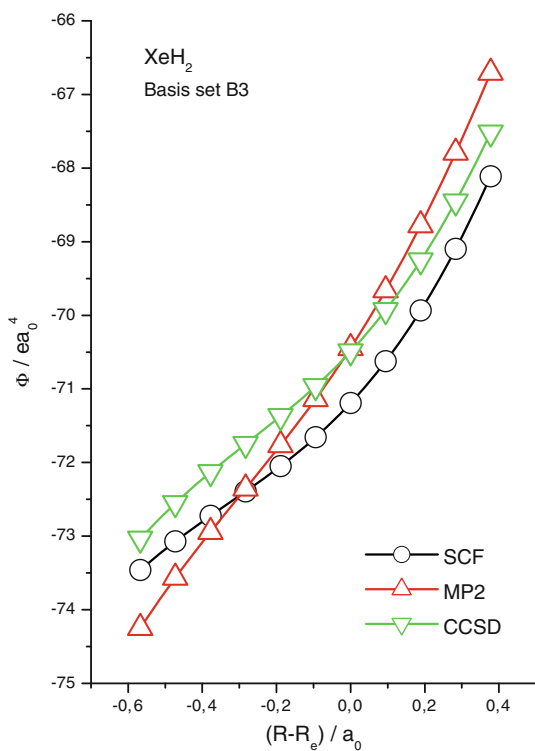


Fig. 2 Xe–H bond length dependence of the hexadecapole moment of XeH_2

Table 3 First derivative (D^1P) of the electric moments of XeH_2 for the symmetric stretch of the Xe–H bond

D^1P	Θ / ea_0	Φ / ea_0^3
SCF	-1.52	5.4
MP2	-0.35	7.8
CCSD	-0.01	5.4

Basis set **B3**

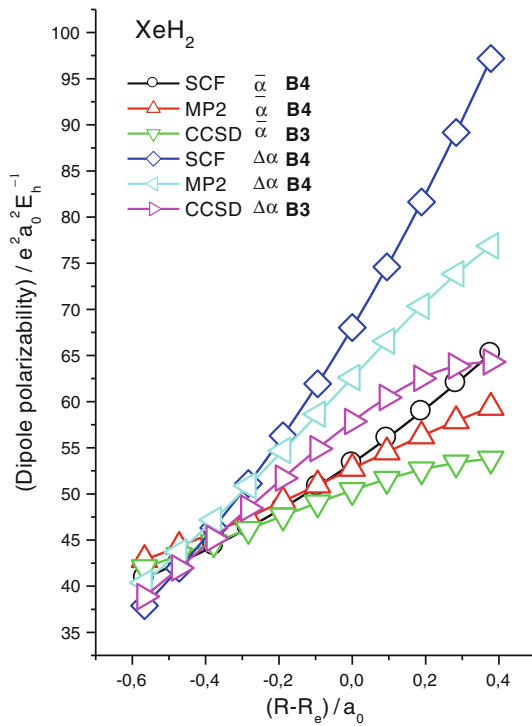
Table 4 Electric polarizability of XeH_2 at the equilibrium molecular geometry

Basis set	Method	α_{zz}	α_{xx}	$\bar{\alpha}$	$\Delta\alpha$
B1	SCF	98.66	29.86	52.79	68.80
	MP2	95.28	31.04	52.45	64.24
	SDQ-MP4	91.10	30.75	50.86	60.36
	MP4	90.57	30.99	50.85	59.58
	CCSD	89.43	30.67	50.26	58.76
	CCSD(T)	87.83	30.89	49.87	56.95
	ECC	-10.83	1.03	-2.92	-11.86
B2	SCF	98.70	30.18	53.02	68.52
	MP2	94.49	31.49	52.49	63.00
	SDQ-MP4	90.35	31.08	50.84	59.27
	MP4	89.84	31.36	50.86	58.48
	CCSD	89.13	31.00	50.38	58.12
	CCSD(T)	87.64	31.24	50.04	56.4
	ECC	-11.06	1.07	-2.98	-12.13
B3	SCF	98.76	30.66	53.36	68.10
	MP2	94.60	31.86	52.77	62.74
	SDQ-MP4	90.12	31.20	50.84	58.92
	MP4	89.68	31.51	50.90	58.16
	CCSD	88.90	31.10	50.37	57.81
	CCSD(T)	87.25	31.32	49.96	55.93
	ECC	-11.51	0.66	-3.40	-12.17
B4	SCF	98.68	30.66	53.33	68.02
	MP2	94.50	31.88	52.75	62.61
	SDQ-MP4	89.97	31.21	50.80	58.76
	MP4	89.53	31.53	50.86	57.99
	CCSD	88.78	31.11	50.33	57.67
	CCSD(T)	87.13	31.34	49.93	55.80
	ECC	-11.55	0.68	-3.40	-12.23
B5	SCF	98.63	30.65	53.31	67.98
	MP2	93.90	31.66	52.41	62.24
B6	SCF	98.63	30.68	53.33	67.95
	MP2	94.99	31.66	52.77	63.33

$D^1\Delta\alpha$ are 27.5 and 66.8, respectively. The MP2 and CCSD values are significantly lower. The CCSD method more than halves the SCF values of $D^1\bar{\alpha}$ and $D^1\Delta\alpha$. Our best CCSD/B3 values are 13.6 ($D^1\bar{\alpha}$) and 29.6 ($D^1\Delta\alpha$).

Table 5 Xe–H bond length dependence of the electric polarizability of XeH_2

$(R-R_e)/\text{\AA}$	$\bar{\alpha}$			$\Delta\alpha$		
	SCF ^a	MP2 ^a	CCSD ^b	SCF ^a	MP2 ^a	CCSD ^b
-0.30	40.90	42.86	42.02	37.89	40.38	38.87
-0.25	42.55	44.29	43.34	41.94	43.70	41.97
-0.20	44.35	45.84	44.73	46.33	47.19	45.18
-0.15	46.33	47.48	46.19	51.11	50.87	48.45
-0.10	48.48	49.19	47.62	56.30	54.70	51.72
-0.05	50.82	50.95	49.04	61.93	58.63	54.89
0	53.33	52.75	50.39	68.02	62.61	57.85
0.05	56.03	54.54	51.60	74.59	66.55	60.45
0.10	58.92	56.27	52.62	81.64	70.33	62.52
0.15	61.98	57.90	53.37	89.17	73.83	63.86
0.20	65.21	59.36	53.78	97.18	76.88	64.30

^a Basis set **B4**^b Basis set **B3****Fig. 3** Xe–H bond length dependence of the mean and the anisotropy of the dipole polarizability of XeH_2

4.3 Dipole hyperpolarizability

We list the calculated hyperpolarizability values as $10^{-3} \times \gamma_{\alpha\beta\gamma\delta}$ in Table 7. Our SCF/B6 values for the Cartesian components are $\gamma_{zzz} = 71.26 \times 10^3$, $\gamma_{xxx} = 7.71 \times 10^3$, and $\gamma_{xxz} = 13.75 \times 10^3$. The dominance of the axial term results in a very large value for the $\Delta_1\gamma$ anisotropy,

Table 6 First derivative (D^1P) of the electric polarizability of XeH_2 for the symmetric stretch of the Xe–H bond

D^1P	$\bar{\alpha}/e^2 a_0 E_h^{-1}$	$\Delta\alpha/e^2 a_0 E_h^{-1}$
SCF ^a	27.6	67.0
MP2 ^a	19.0	42.1
CCSD ^b	13.6	29.6

^a Basis set B4^b Basis set B3**Table 7** Electric hyperpolarizability of XeH_2 at the equilibrium molecular geometry (all values are given as $10^{-3} \times \gamma_{\alpha\beta\gamma\delta}$)

Basis set	Method	γ_{zzz}	γ_{xxx}	γ_{xxz}	$\bar{\gamma}$	$\Delta_1\gamma$	$\Delta_1\gamma$
B1	SCF	70.42	6.03	8.71	24.27	213.28	24.16
	MP2	91.17	8.31	10.04	30.70	270.38	39.23
	SDQ-MP4	92.74	7.19	9.19	29.74	277.03	44.79
	MP4	94.99	7.67	9.40	30.61	282.47	46.28
	CCSD	92.37	7.12	8.67	29.21	274.68	47.45
	CCSD(T)	93.86	7.50	8.65	29.69	277.56	49.44
B2	ECC	23.44	1.46	-0.06	5.42	64.27	25.28
	SCF	68.13	6.24	9.36	24.44	207.52	18.21
	MP2	89.22	8.43	11.32	31.40	267.92	29.71
	SDQ-MP4	87.42	7.35	10.13	29.51	263.25	33.99
	MP4	90.17	7.85	10.45	30.58	270.47	35.33
	CCSD	86.78	7.03	9.61	28.79	261.03	36.17
B3	CCSD(T)	88.75	7.39	9.69	29.44	265.74	38.01
	ECC	20.62	1.15	0.33	5.00	58.23	19.8
	SCF	67.77	6.85	12.80	27.45	214.29	-2.14
	MP2	88.56	8.91	15.53	34.89	276.61	4.31
	SDQ-MP4	85.79	7.68	13.16	31.78	266.12	14.53
	MP4	89.15	8.25	13.78	33.26	275.78	14.70
B4	CCSD	85.20	7.41	12.43	30.94	263.28	18.02
	CCSD(T)	87.76	7.86	12.63	31.85	269.76	19.85
	ECC	19.99	1.00	-0.17	4.40	55.47	21.99
	SCF	71.34	7.60	13.58	29.18	224.33	-2.52
	MP2	92.64	8.52	15.44	35.42	290.20	8.51
	SDQ-MP4	88.00	6.81	12.72	31.40	274.92	18.50
B5	MP4	91.55	7.38	13.32	32.90	285.07	19.04
	CCSD	87.71	6.64	12.06	30.73	272.79	21.97
	CCSD(T)	90.11	6.82	12.00	31.26	279.07	24.93
	ECC	18.77	-0.79	-1.58	2.07	54.74	27.45
	SCF	71.18	7.50	13.66	29.16	224.54	-3.26
	MP2	90.01	9.56	15.65	35.62	278.72	5.66
B6	SCF	71.26	7.71	13.75	29.36	224.18	-3.52
	MP2	91.43	10.31	16.16	36.71	281.55	4.79

224.18×10^3 , while the $\Delta_2\gamma$ one is quite small at -3.52 . Our SCF and post-Hartree–Fock results calculated with basis **B4** show that the γ_{zzz} component increases considerably by the introduction of electron correlation. For γ_{xxx} and γ_{xxz} , the

Table 8 DFT values of XeH_2 calculated with basis set **B4**

Method	α_{zz}	α_{xx}	$\bar{\alpha}$	$\Delta\alpha$
B3LYP	92.67	32.03	52.25	60.64
B3PW91	91.69	31.56	51.61	60.13
mPW1PW91	92.00	31.49	51.66	60.50

Table 9 DFT values of XeH_2 calculated with basis set **B4** (all values are given as $10^{-3} \times \gamma_{z\beta\gamma\delta}$)

Method	γ_{zzzz}	γ_{xxxx}	γ_{xxzz}	$\bar{\gamma}$	$\Delta_1\gamma$	$\Delta_2\gamma$
B3LYP	100.22	11.51	17.54	40.21	307.25	6.47
B3PW91	97.78	10.08	16.12	37.23	292.38	8.16
mPW1PW91	91.36	10.11	16.15	36.58	282.12	4.58

effect is small and negative. Overall, electron correlation has a small effect on the mean hyperpolarizability $\bar{\gamma}$ and a rather large one on the anisotropies $\Delta_1\gamma$ and $\Delta_2\gamma$. The evolution of the CCSD(T) values seems particularly smooth for the mean hyperpolarizability.

4.4 DFT values and comparison to ab initio results

B3LYP, B3PW91, and mPW1PW91 values for the dipole polarizability and hyperpolarizability of XeH_2 calculated with basis set **B4** are given in Tables 8 and 9. The DFT results are well grouped. Their comparison to conventional ab initio methods can be gleaned from Figs. 4 and 5. For the mean polarizability (Fig. 4), DFT methods are included in the range of values between MP2 and MP3. For the hyperpolarizability (Fig. 5), DFT methods seem to overestimate $\bar{\gamma}$.

In Table 10, we show the calculated similarity values $S(i,j)$ for all methods SCF, MP2, MP3, SDQ-MP4, MP4, CCSD, CCSD(T), B3LYP, B3PW91, and mPW1PW91. The similarity is calculated for a theoretical description that includes all Cartesian components of the (hyper)polarizability. The most dissimilar methods are SCF and B3LYP, $S(\text{SCF}, \text{B3LYP}) = 0$. The clustering of the theoretical methods is more obvious in Fig. 6. Overall, the minimum spanning tree (MST) shows that DFT methods are distinct from conventional ab initio ones. Removing from the MST all edges that larger than a threshold value $D_T = 0.5$, we see that the space of theoretical descriptions clusters as

$$\begin{aligned} \text{TD} &= \{\text{SCF}\} \cup \{\text{MP2}\} \\ &\cup \{\text{MP3, SDQ - MP4, MP4, CCSD, CCSD(T)}\} \\ &\cup \{\text{B3LYP, B3PW91, mPW1PW91}\} \end{aligned}$$

Lowering the threshold to $D_T = 0.2$ leads to a further split of the DFT cluster to

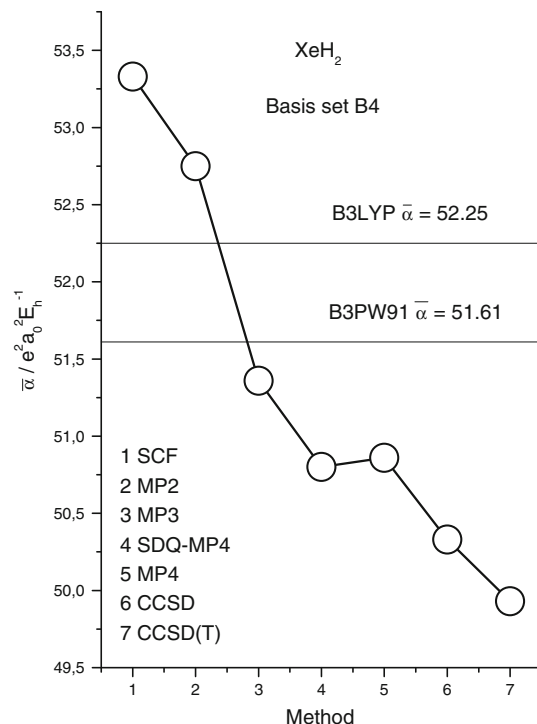
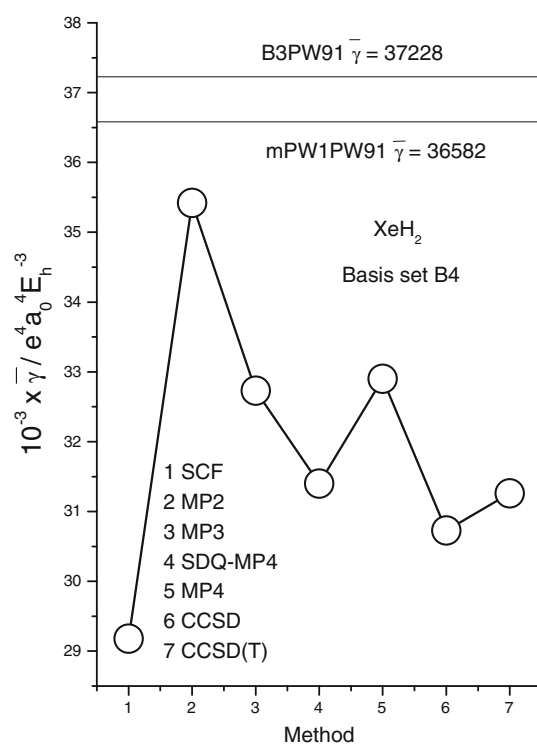
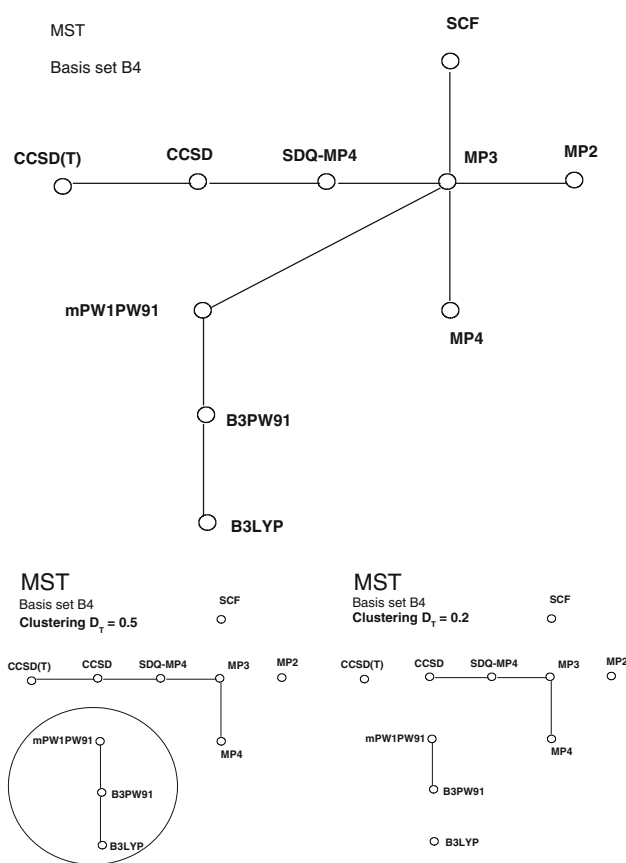
**Fig. 4** Comparison of ab initio and DFT method for the mean dipole polarizability of XeH_2 **Fig. 5** Comparison of ab initio and DFT method for the mean dipole hyperpolarizability of XeH_2

Table 10 Similarity $S(i,j)$ between the performance of ab initio and DFT methods over the (hyper)polarizability of XeH_2 calculated with basis set B4

	SCF	MP2	MP3	SDQ-MP4	MP4	CCSD	CCSD(T)	B3LYP	B3PW91	mPW1PW91
SCF	1	0.53485	0.59416	0.58659	0.50868	0.55581	0.45976	0	0.12043	0.14101
MP2	0.53485	1	0.78307	0.69664	0.75784	0.63750	0.63706	0.15684	0.21688	0.22324
MP3	0.59416	0.78307	1	0.91357	0.91384	0.85379	0.82526	0.13091	0.23172	0.24141
SDQ-MP4	0.58659	0.69664	0.91357	1	0.88548	0.9389	0.87246	0.10608	0.22073	0.23151
MP4	0.50868	0.75784	0.91384	0.88548	1	0.84836	0.87911	0.13349	0.22861	0.23553
CCSD	0.55581	0.63750	0.85379	0.93890	0.84836	1	0.89333	0.08644	0.20820	0.21910
CCSD(T)	0.45976	0.63706	0.82526	0.87246	0.87911	0.89333	1	0.09685	0.20669	0.21387
B3LYP	0	0.15684	0.13091	0.10608	0.13349	0.08644	0.09685	1	0.81273	0.79036
B3PW91	0.12043	0.21688	0.23172	0.22073	0.22861	0.20820	0.20669	0.81273	1	0.96752
mPW1PW91	0.14101	0.22324	0.24141	0.23151	0.23553	0.21910	0.21387	0.79036	0.96752	1

**Fig. 6** Minimum spanning tree (MST) and clustering for the theoretical descriptions of XeH_2 calculated with basis B4

$$\begin{aligned} & \{ \text{B3LYP}, \text{B3PW91}, \text{mPW1PW91} \} \\ &= \{ \text{B3LYP} \} \cup \{ \text{B3PW91}, \text{mPW1PW91} \}. \end{aligned}$$

5 Conclusions

We have reported electric multipole moments and dipole (hyper)polarizability values for xenon hydride using conventional ab initio methods and DFT-based approaches.

We have employed a sequence of large, flexible Gaussian-type basis sets. Basis set effects were studied both at the SCF and post-Hartree–Fock levels of theory. Our best values for the quadrupole and hexadecapole moment were obtained at the CCSD/B4 level of theory and are $\Theta = -4.8760 \text{ } ea_0^2$ and $\Phi = -71.95 \text{ } ea_0^4$. Our best values for the invariants of the (hyper)polarizability were obtained at the CCSD(T)/B4 level of theory. They are $\bar{\alpha} = 49.93$ and $\Delta\alpha = 55.80 \text{ } e^2 a_0^2 E_h^{-1}$, for the mean and the anisotropy of the dipole polarizability, respectively. For the second hyperpolarizability, we obtain $\bar{\gamma} = 31.26$, $\Delta_1\gamma = 279.07$ and $\Delta_1\gamma = 24.93 \times 10^3 \times e^4 a_0^4 E_h^{-3}$, for the mean and the anisotropies. Due to the large longitudinal components, both properties are very anisotropic.

A quantitative analysis of the performance of three widely used DFT-based methods, B3LYP, B3PW91, and mPW1PW91, shows that the calculated dipole polarizability is comparable to that obtained by conventional ab initio methods, but the magnitude of the second hyperpolarizability is overestimated. Overall, the DFT methods lead to very similar, well grouped, theoretical descriptions of XeH_2 .

References

- Pettersson M, Lundell J, Räsänen M (1995) J Chem Phys 102:6423
- Khrachtchev L, Tanskanen H, Lundell J, Pettersson M, Kiljunen H, Räsänen M (2003) J Am Chem Soc 125:4696
- Gerber RB (2004) Annu Rev Phys Chem 55:55
- Lundell J, Cohen A, Gerber RB (2002) J Phys Chem A 106:11950 (and references therein)
- Avramopoulos A, Serrano-Andrés L, Li J, Reis H, Papadopoulos MG (2007) J Chem Phys 127:214102
- Maroulis G (2008) J Chem Phys 129:044314 (and references therein)
- Nahler NH, Baumfalk R, Buck U, Bihary Z, Gerber RB, Friedrich B (2003) J Chem Phys 119:224
- Pettersson M, Lundell J, Räsänen M (1995) J Chem Phys 103:205

9. Lundell J, Khriachtchev L, Pettersson M, Räsänen M (2000) Low Temp Phys 26:680
10. Lorenz M, Räsänen M, Bondybey VE (2009) J Phys Chem A 104:3770
11. Khriachtchev L, Pettersson M, Tanskanen H, Räsänen M (2002) Chem Phys Lett 359:135
12. Feldman VI, Kobzarenko AV, Baranova IA, Danchenko AV, Sukhov FF, Tsivion E, Gerber RB (2009) J Chem Phys 131:161101
13. Runeberg N, Seth M, Pyykkö P (1995) Chem Phys Lett 246:239
14. Lundell J, Berski S, Latajka Z (2000) Phys Chem Chem Phys 2:5521
15. Solimannejad M, Mohammadi Amlashi L, Alkorta I, Elguero J (2006) Chem Phys Lett 422:226
16. Lundell J, Berski S, Latajka Z (2003) Chem Phys Lett 371:295
17. Takayanagi T, Asakura T, Takahashi K, Taketsugu Y, Taketsugu T, Noro T (2007) Chem Phys Lett 446:14
18. Blanco F, Solimannejad M, Alkorta I, Elguero J (2008) Theor Chem Account 121:181
19. Solimannejad M, Malekani M, Alkorta I (2010) J Mol Struct (THEOCHEM) 955:140
20. Birnbaum G (ed) (1985) Phenomena induced by intermolecular interactions. Plenum, New York
21. Hanna DC, Yuratich MA, Cotter D (1979) Nonlinear optics of free atoms and molecules. Springer, Berlin
22. Tabisz GC, Neuman MN (eds) (1995) Collision- and interaction-induced spectroscopy. Kluwer, Dordrecht
23. Gray CG, Gubbins KE (1984) Theory of molecular fluids. Clarendon, Oxford
24. Berkowitz M, Parr RG (1988) J Chem Phys 88:2554
25. Vela A, Gázquez JL (1990) J Am Chem Soc 112:1490
26. Liu PH, Hunt KLC (1995) J Chem Phys 103:10597
27. Torrent-Sucarrat M, De Proft F, Geerlings P (2005) J Phys Chem A 109:6071
28. Donald KJ (2006) J Phys Chem A 110:2283
29. Handy NC, Schaefer HF III (1984) J Chem Phys 81:5031
30. Maroulis G, Bishop DM (1986) J Phys B 19:369
31. Maroulis G, Thakkar AJ (1990) J Chem Phys 92:812
32. Maroulis G, Makris C, Hohm U, Goebel D (1997) J Phys Chem A 101:953
33. Maroulis G, Pouchan C (2003) J Phys Chem B 107:10683
34. Karamanis P, Maroulis G, Pouchan C (2006) Chem Phys 331:19
35. Maroulis G, Haskopoulos A (2002) Chem Phys Lett 358:64
36. Maroulis G, Xenides D (2003) J Phys Chem A 107:712
37. Maroulis G (2003) J Phys Chem A 107:6495
38. Hohm U, Maroulis G (2004) J Chem Phys 121:10411
39. Maroulis G (1995) Int J Quant Chem 55:173
40. Maroulis G (1998) J Chem Phys 108:5432
41. Maroulis G (1999) J Chem Phys 111:583
42. Maroulis G (2000) J Chem Phys 113:1813
43. Christodouleas C, Xenides D, Simos TE (2010) J Comput Chem 31:412
44. Xenides D, Karamanis P, Pouchan C (2010) Chem Phys Lett 498:134
45. Buckingham AD (1967) Adv Chem Phys 12:107
46. McLean AD, Yoshimine M (1967) J Chem Phys 47:1927
47. Maroulis G (1992) Chem Phys Lett 199:250
48. Szabo A, Ostlund NS (1982) Modern quantum chemistry. McMillan, New York
49. Wilson S (1984) Electron correlation in molecules. Clarendon, Oxford
50. Urban U, Cernusak I, Kellö V, Noga J (1987) Methods Comput Chem 1:117
51. Helgaker T, Jørgensen P, Olsen J (2000) Molecular electronic-structure theory. Wiley, Chichester
52. Frisch MJ, Trucks GW, Schlegel HB et al (2004) GAUSSIAN 03, Revision D.01. Gaussian Inc., Wallingford
53. Maroulis G, Xenides D (2005) Comp Lett 1:246
54. Chatrand G, Lesniak L (1986) Graphs and digraphs. Wadsworth, Belmont
55. Spath H (1980) Cluster analysis algorithms. Ellis Horwood, Chichester, p 1980
56. Davidson ER, Feller D (1986) Chem Rev 86:681
57. Arruda PM, Canal Neto A, Jorge FE (2009) Int J Quant Chem 109:1189
58. Baranowska A, Sadlej AJ (2010) J Comput Chem 31:552
59. Maroulis G, Bishop DM (1985) Chem Phys Lett 114:182
60. Maroulis G, Bishop DM (1986) Mol Phys 58:273
61. Maroulis G, Bishop DM (1986) Mol Phys 57:359
62. Maroulis G, Pouchan C (1998) Phys Rev 57:2440
63. Maroulis G, Thakkar AJ (1991) J Chem Phys 95:9060
64. Maroulis G (1996) Chem Phys Lett 259:654
65. Maroulis G, Xenides D (1999) J Phys Chem A 103:4590
66. Maroulis G, Pouchan C (2003) Phys Chem Chem Phys 5:1992
67. Maroulis G, Haskopoulos A (2006) Chem Phys Lett 428:28
68. Maroulis G, Haskopoulos A (2001) Chem Phys Lett 349:335
69. Maroulis G (2000) J Phys Chem A 104:4772
70. Maroulis G, Haskopoulos A, Xenides D (2004) Chem Phys Lett 396:59
71. <ftp://ftp.chemie.uni-karlsruhe.de/pub>
72. Maroulis G, unpublished results
73. Bancewicz T, Glaž W, Godet JL, Maroulis G (2008) J Chem Phys 129:124306
74. Haskopoulos A, Maroulis G (2010) Chem Phys 367:127